J Therm Anal Calorim (2011) 103:821–826
DOI 10.1007/s10973-010-1042-z

A complete thermo-mechanical study of a NiTiCu shape memory alloy wire

Adelaide Nespoli · Stefano Besseghini

Received: 29 July 2010 / Accepted: 7 September 2010 / Published online: 21 September 2010

Abstract Shape memory alloy mechanical performance and phase transformation temperatures depend on the composition of the alloy, on the thermo-mechanical history, and on the applied load. For this reason is important to execute a deep investigation of the SMA material before its final use. In this study we investigate the thermo-mechanical behavior of a NiTiCu wire under stress-free condition through the differential scanning calorimetry and the electrical resistance measurements and under load through tensile and hysteresis tests. The phase transformation temperature dependence on the applied load, by means of the Clausius–Clapeyron equation, as well as on the thermal treatment temperature are also studied.

Keywords NiTiCu · DSC · Electrical resistance · Hysteresis test · Heat treatment

Introduction

Shape memory alloys (SMAs) have two crystalline structures, martensite and austenite, stable at two different temperatures. Consequently, the material is sensitive to a specific thermal cycle transforming from austenite to martensite during cooling and from martensite to austenite during heating. The critical temperatures at which each phase starts and finishes depend on the composition of the alloy, on the thermo-mechanical history, and on the applied load.

A. Nespoli (✉) · S. Besseghini
Consiglio Nazionale delle Ricerche, Istituto per l'Energetica e le Interfasi (CNR-IENI), UOS di Lecco, Corso Promessi Sposi 29, 23900 Lecco, Italy
e-mail: a.nespoli@ieni.cnr.it

NiTi and NiTi-based systems are the most common SMAs; they show pseudoelasticity, high damping capacities, ductility, strength, fatigue, and corrosion resistance. The addition of a third element to the NiTi system is often used to modify the transformation temperatures; usually a change on the transformation path is also observed [1, 2].

The addition of Cu for Ni in the equiatomic NiTi system reduces the sensitivity of the transformation temperatures to the chemical composition and to the thermal treatment time; diminishes the thermal hysteresis; reduces the mechanical hysteresis in the pseudoelastic regime; enhances the thermo-mechanical cycling stability [1]. This alloy goes through different transformation sequences when Cu concentration is varied in some specific limits: ternary alloy containing up to 5–7 at% of Cu undergoes through the B2–B19′ transformation; for Cu content belonging to the 7–16 at% range the alloy shows the two-stage B2–B19–B19′ transformation; for Cu concentration higher than 16 at% the ternary alloy exhibits the B2–B19 transformation (B2, B19, and B19′ represent the cubic, the orthorhombic, and the monoclinic structures, respectively) [3].

Before starting any new application an SMA element should be deeply characterized in order to assess its behavior under stress-free and under load conditions [4–7]. The first information which rises out of these characterizations is about the phase transformation temperatures (PTT), which vary as a function of the applied load as described by the Clausius–Clapeyron law [1]. The thermal treatment also play an important role in determine the SMA transformation temperatures and its final thermo-mechanical performance [8, 9].

There are many techniques which are currently employed to characterize an SMA [10, 11]. The most common are the ones which allow to detect the PTT under stress-free condition, i.e., differential scanning calorimetry

(DSC) and electrical resistance (ER) measurements [12–16], and the ones which characterize the specimen under load, for example, the tensile and hysteresis tests [17, 18].

In this study we investigate the thermo-mechanical behavior of a commercial NiTiCu wire using differential scanning calorimetry, electrical resistance measurements, and tensile tests. The influence of the thermal history and the applied load on the transformation temperatures is studied as well.

Experimental

This study concerns the thermo-mechanical characterization of a commercial NiTiCu wire having the diameter of 0.8 mm. The wire was first analyzed through an Energy Dispersive X-Ray Spectrometer (EDS) INCA ENERGY 200 (Oxford Instruments) in connection with a scanning electron microscopy (SEM LEO 1430) in order to assess its elemental composition. Three sites of interest and three spectra for each site were tested.

Several samples were then thermal treated at different temperatures, 400, 450, 500, 550 °C for 30′ and 750 °C for 15′ (after the heat treatment each sample was water quenched).

The samples were subsequently subject to a series of thermo-mechanical tests. The first set of experiments concerns the thermal analysis in the stress-free condition through the differential scanning calorimetry (DSC) and electrical resistance (ER) measurements. DSC measures were made using a DSC/220 Seiko Instruments Inc. device equipped with a liquid nitrogen cooling system. The temperature range for the DSC measurement was from −50 to 100 °C under the controlled heating/cooling rate of 10 °C/min. ER analysis was made using a Resistomat® 2305 device in the four-probe mode; each NiTiCu sample was immersed in a thermostatic bath (Lauda Ecoline RE306) containing Krio20® silicon oil, and subjected to the thermal cycles from −35 to 130 °C with a heating/cooling rate of 1 °C/min.

With the second set of tests we studied the NiTiCu sample mechanical response under load. First, a commercial MTS 2/M thermo-mechanical testing machine (MTS Systems, S.r.l.) equipped with a thermal camera was used to assess the austenite and the martensite mechanical behavior separately. An additional mechanical test was then made on the sample treated at 450 °C, by studying its thermal hysteresis under different loads. For this purpose a linear variable displacement transducer (LVDT) DC50 (Solartron Metrology) was employed to monitor the stroke of the SMA wire during the phase transformation. The wire was heated by Joule effect (3 A for 30 s) and the loads were fixed to the free end in a way that the uniaxial tensile state on the SMA wire was always assured. Three thermocouples (K type) were used to record the wire temperature during the test, fixed to the wire and insulated as respect to the surrounding temperature. A fourth K-thermocouple was employed to register the nearby temperature. With this last test the Clausius–Clapeyron coefficient was derived. The maximum stroke dependence on the applied electrical current and on the heating time is finally studied.

Results and discussion

Energy Dispersive X-Ray Spectrometer analysis result shows that the NiTiCu sample has the following mean elemental composition: 51.20Ti–43.49Ni–5.31Cu.

In Fig. 1 are reported DSC and ER curves as a function of the thermal treatment temperature. DSC curves change strongly depending on the thermal treatment temperature. We can see one clear peak both on cooling and on heating; the area under this peak represents the B2–B19′ and the B19′–B2 phase transformation latent heat, respectively [19, 20]. This peak is almost spread for low thermal treatment temperatures and becomes sharper with the increase of the temperature, meaning that the range of temperature in which the two phases coexist becomes smaller for high treatment temperatures.

The ER curves hardly change and show a low increasing of the electrical resistance rate during the B2–B19′ and the B19′–B2 transformations. On cooling, the ER curves show one minimum and one maximum; the temperatures at which we find these two limits represent the B2–B19′ starting (Ms) and finishing (Mf) temperatures, respectively. Between these two limits the two phases coexist.

The PTT can be derived from both the two techniques using the tangent method [17]; we find low discrepancies between them which are mainly due to the different heating/cooling rates used during test [21, 22]. The trend of the PTT as a function of the thermal treatment temperatures is reported in Fig. 2, where the B2–B19′ starting and finishing temperatures, Ms and Mf, and the B19′–B2 starting and finishing temperatures, As and Af, were derived from the DSC curves. In this picture is also reported the transformation enthalpy normalized to the sample mass. The PTT increase regularly till the 550 °C thermal treatment temperature; after this value they remain constant. This behavior happens because the internal stresses generated by the dislocations produced by the working process, which restrict the martensite from transforming into austenite for low treatment temperatures, are completely removed for high treatment temperatures. As regard the NiTiCu alloy, we can state that the treatment conducted at 550 °C is enough to remove all the internal stresses as the

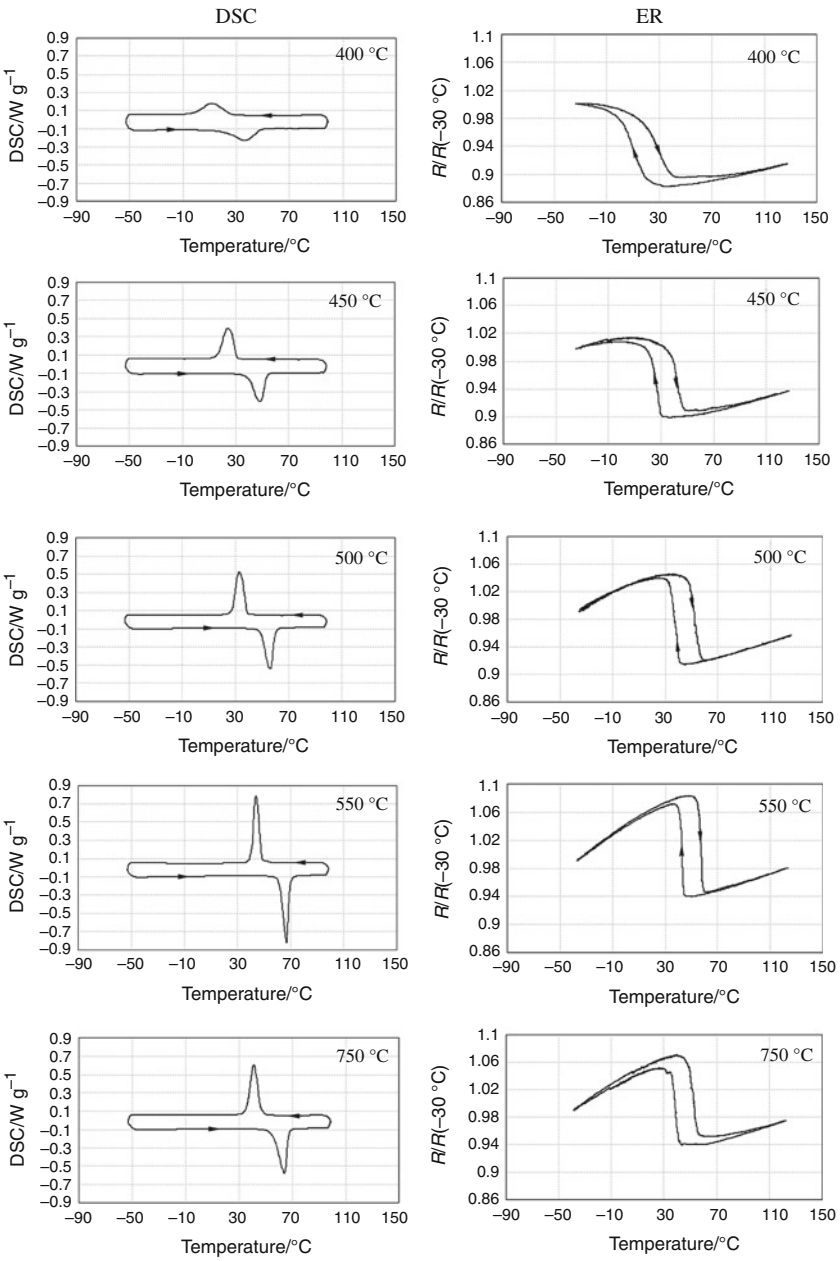

Fig. 1 Pure thermal test results. ER (*on the right*) and DSC (*on the left*) curves for different thermal treatment temperatures, 400, 450, 500, 550 °C for 30 min and 750 °C for 15 min (samples were water quenched after each heat treatment); heating/cooling rate was set to 10 and 1 °C/min for DSC and ER measurements, respectively

DSC curve of the sample treated at this temperature is similar to the fully annealed one (i.e., 750 °C). An analogous trend is visible for the transformation enthalpy, where the upper limit is very similar to the NiTi system one [23].

In Fig. 3 is reported the mechanical response as a function of the thermal treatment temperatures, both of austenite (a) and of martensite (b). The loading plateau decreases with the increase of the thermal treatment temperature, and the pseudoelastic flag shape [1, 2] is visible only for the samples treated at low temperatures. A general decreasing of the performance as the thermal treatment temperature increases was observed. As for the pure thermal test, the specimens treated at 550 and at 750 °C show an analogous mechanical behavior.

Figure 4a shows the hysteresis tests under nine different loads of the sample thermal heated at 450 °C; Fig. 4b illustrates the stress–stroke curves derived from both the MTS and the LVDT analyses, where the stroke derived from the MTS test was calculated as the difference between the martensite and the austenite deformation at an identical applied load. We can see that the stroke increases with the increasing of the applied load and it reaches a maximum at about 138 MPa; after this value the stroke remains constant. It is important to notice that LVDT and MTS results

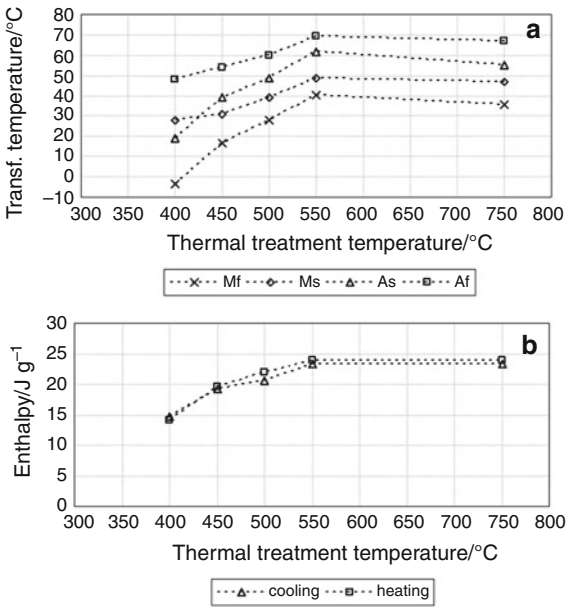

Fig. 2 DSC analysis results. PTT (**a**) and enthalpy normalized to the mass (**b**) as a function of the thermal treatment temperature

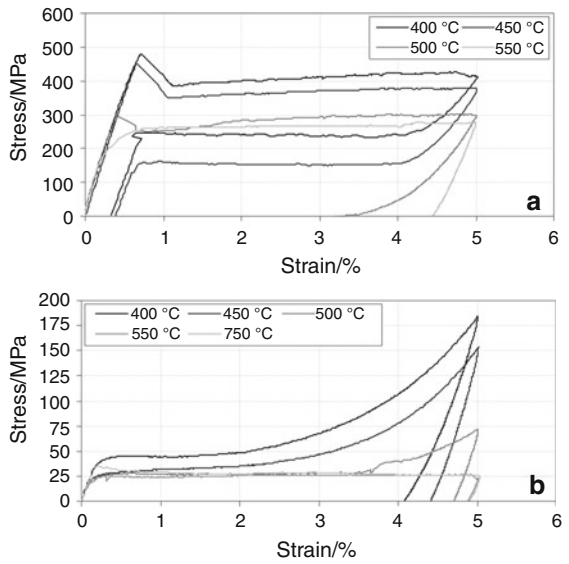

Fig. 3 MTS tensile test results. Stress versus strain as a function of the thermal treatment temperature for austenite (**a**) and martensite (**b**)

almost overlapped each other meaning that they give similar results even though the way of heating the wire during the two tests is different as we use Joule effect for LVDT test and convection for MTS one.

From the hysteresis cycles conducted at different loads we estimated the PTT by means of the tangent method and plotted in the stress–temperature plane the trend of the stress as a function of each transition temperature, see Fig. 5. Each transformation temperature increases with the

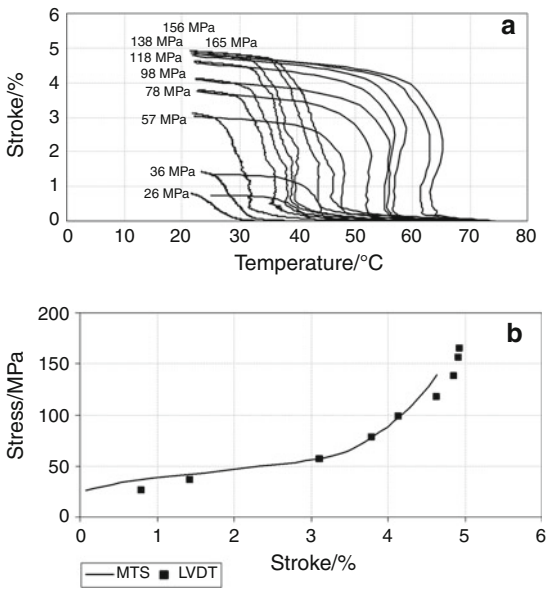

Fig. 4 LVDT tensile test results on the sample treated at 450 °C for 30 min and water quenched. **a** Thermo-mechanical hysteresis under different loads; **b** comparison between the stress–stroke data derived from the MTS and the LVDT tensile tests

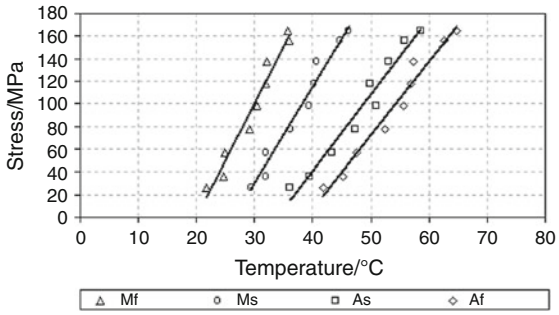

Fig. 5 Stress versus phase transformation temperature. The rate dσ/dT of each line represents the Clausius–Clapeyron coefficient

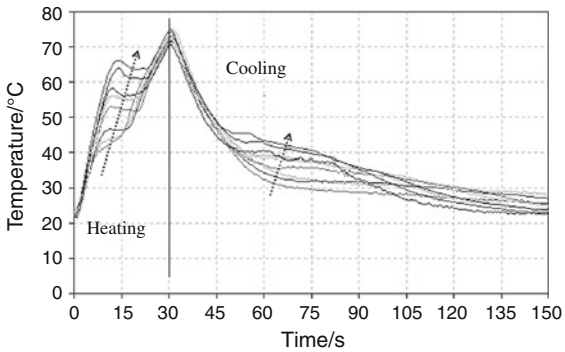

Fig. 6 Sample temperature for different loads registered during the hysteresis tests (*arrows* indicate the increasing direction of load)

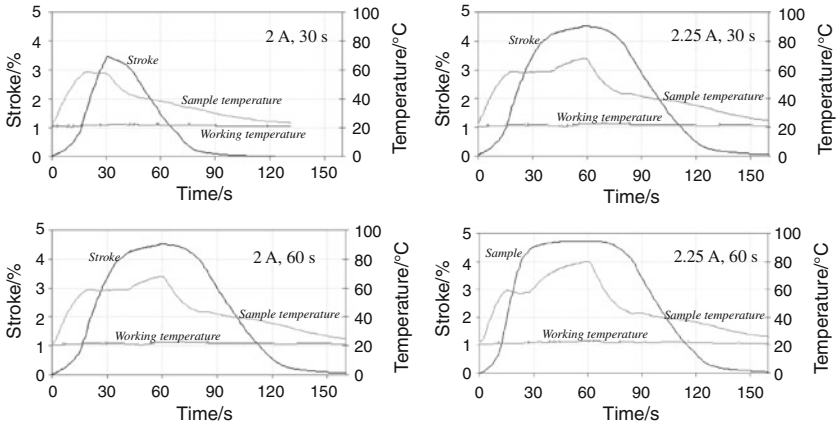

Fig. 7 Current effects on stroke (*black lines*) and on sample temperature (*gray lines*). The electro-thermal activation was made under different currents, 2 A and 2.25 A, and different activation times, 30 and 60 s

increasing of stress with rate $d\sigma/dT$ equal to the Clausius–Clapeyron coefficient: 9.98 MPa/°C for Mf, 8.55 MPa/°C for Ms, 6.76 MPa/°C for As, and 6.49 MPa/°C for Af.

The increasing of the PTT as a function of the applied load is visible also in the sample temperature registered during the hysteresis tests conducted under the nine different loads reported in Fig. 4. In Fig. 6 we can observe that each temperature curve shows two nearly flat segments, more visible during heating, in which the phase transformation takes place. The temperatures corresponding to the starting and finishing points of each segment coincide with the PTT and shift to higher values with the increasing of the load both during heating and cooling (arrows indicate the load increasing direction).

Figure 7 shows the influence of the activation current and the activation time on the stroke and on the temperature of the sample thermal treated at 450 °C and stressed with 116 MPa. We considered four cases in which we varied the activation current and time: (A) current of 2 A for 30 s, (B) current of 2 A for 60 s, (C) current of 2.25 A for 30 s, and (D) current of 2.25 A for 60 s. The sample temperature was estimated by calculating the average value deriving from three thermocouples; during the test the working temperature was also registered. We can see that the specimen reaches a maximum stroke of 4.8% with a current of 2.25 A for 60 s; a similar result is obtained by providing the same current for 30 s and by supplying a current of 2 A for 60 s. Analyzing the sample temperature we can observe that it undergoes to overheating in all cases except the (A) one: the sample mean temperature reaches 80 °C with a current of 2.25 A for 60 s and about 70 °C with a current of 2 A for 60 s and 2.25 A for 30 s. The sample heated with a current of 2 A for 30 s never reaches the Af temperature; for this reason it does not complete the phase transformation as we can see also from the maximum stroke it achieves. During the tests the mean working temperature was around 20 °C.

Conclusions

A commercial NiTiCu wire was analyzed through pure thermal and thermo-mechanical tests. The results show a strict relationship between the whole performance and thermal state of the wire. As the phase transformation temperatures change as a function of the applied load, it is important to know the exact final application of the wire in order to establish a correct thermal process and to obtain the desired thermo-mechanical characteristics. An accurate measurement of the sample temperature is fundamental to avoid overheating and to adjust the final stroke.

References

1. Funakubo H. Shape memory alloys. London: Gordon and Breach Science Publishers; 1984.
2. Otsuka K, Wayman CM. Shape memory materials. Cambridge: Cambridge University Press; 1998.
3. Nam TH, Saburi T, Nakata Y, Shimizu K. Shape memory characteristics and lattice deformation in Ti–Ni–Cu alloy. Mater Trans. 1990;31:1050–6.
4. Degeratu S, Rotaru P, Manolea Gh, Manolea HO, Rotaru A. Thermal characteristics of Ni–Ti SMA (shape memory alloy) actuators. J Therm Anal Calorim. 2009;97:695–700.
5. Torra V, Auguet C, Isalgue A, Lovey FC, Sepulveda A, Soul H. Metastable effects on martensitic transformation in SMA. Part VIII Temperature effects on cycling. J Therm Anal Calorim. 2009. doi:10.1007/s10973-009-0613-3.
6. Carreras G, Isalgue A, Torra V, Lovey FC, Soul H. Metastable effects on martensitic transformation in SMA. Part V. Fatigue-life and detailed hysteresis behavior in NiTi and Cu-based alloys. J Therm Anal Calorim. 2008;91(2):575–9.
7. Auguet C, Isalgue A, Lovey FC, Pelegrina JL, Ruiz S, Torra V. Metastable effects on martensitic transformation in SMA. Part III. Tentative temperature effects in a NiTi alloy. J Therm Anal Calorim. 2007;89(2):537–42.
8. Miller DA, Lagoudas DC. Influence of cold work and heat treatment on the shape memory effect and plastic strain development of NiTi. Mater Sci Eng A. 2001;308:161–75.

9. Fukuda T, Kakeshita T, Kitayama M, Saburi T. Effect of aging on martensitic transformation in a shape memory Ti–40.5Ni–10Cu alloy. J Phys IV. 1995;5:717–22.
10. Uchil J. Shape memory alloys—characterization techniques. J Phys. 2002;58:1131–9.
11. Duerig TW, Melton KN, Stockel D, Wayman CM. Engineering aspects of shape memory alloys. London: Butterworth-Heinemann; 1990.
12. Auguet C, Isalgue A, Torra V, Lovey FC, Pelegrina JL. Metastable effects on martensitic transformation in SMA. PartVII Aging problems in NiTi. J Therm Anal Calorim. 2008;92:63–71.
13. Artiaga R, García A, García L, Varela A, Mier JL, Naya S, Gra M. DMTA study of a nickel-titanium wire. J Therm Anal Calorim. 2002;70:199–207.
14. Lo YC, Wu SK, Horng HE. A study of B2-B19-B19′ two-stage martensitic transformation in a Ti50Ni40Cu10 alloy. Acta Metall Mater. 1993;41:747–59.
15. Uchil J, Mohanchandra KP, Ganesh Kumara K, Mahesh KK. Study of critical dependence of stable phases in nitinol on heat treatment using electrical resistivity probe. Mater Sci Eng A. 1998;251:58–63.
16. Wu SK, Lin HC, Lin TY. Electrical resistivity of Ni–Ti binary and Ti–Ni-X (X = Fe, Cu) ternary shape memory alloys. Mater Sci Eng A. 2006;438–440:536–9.
17. Shaw JA, Kyriakides S. Thermomechanical aspects of NiTi. J Mech Phys Solids. 1995;43:1243–81.
18. Marony Sousa Farias Nascimento M, de Araújo CJ, da Rocha Neto JS, Nogueira de Lima AM. Electro-thermomechanical characterization of Ti–Ni shape memory alloy thin wires. Mater Res. 2006;9:15–9.
19. Nam TH, Saburi T, Shimizu K. Cu-content dependence of shape memory characteristics in Ti–Ni–Cu alloys. Mater Trans. 1990;31:956–67.
20. Otsuka K, Ren X. Physical metallurgy of Ni–Ti-based shape memory alloys. Prog Mater Sci. 2005;50:511–678.
21. Wang ZG, Zu XT, Huo Y. Effect of heating/cooling rate on the transformation temperatures in NiTiCu shape memory alloys. Thermochim Acta. 2005;436:153–5.
22. Nurveren K, Akdoğan A, Huang WM. Evolution of transformation characteristics with heating/cooling rate in NiTi shape memory alloys. J Mater Process Technol. 2008;196:129–34.
23. Wang G, Jiang XX, Nikanpour D. Measurement of specific heat, latent heat and phase transformation temperatures of shape memory alloys. High Temp High Press. 2008;37:91–107.